NASA Contractor Report 4002

A Study of the Stress Wave Factor Technique for Nondestructive Evaluation of Composite Materials

A. Sarrafzadeh-Khoee, M. T. Kiernan,
J. C. Duke, Jr., and E. G. Henneke II

GRANT NAG3-172
JULY 1986

NASA

NASA Contractor Report 4002

A Study of the Stress Wave Factor Technique for Nondestructive Evaluation of Composite Materials

A. Sarrafzadeh-Khoee, M. T. Kiernan,
J. C. Duke, Jr., and E. G. Henneke II
Virginia Polytechnic Institute and State University
Blacksburg, Virginia

Prepared for
Lewis Research Center
under Grant NAG3-172

National Aeronautics
and Space Administration

**Scientific and Technical
Information Branch**

1986

This Page Intentionally Left Blank

Abstract

This interim report updates the reported findings under NASA Grant 3-172. Included are descriptions of a novel optical in-plane/out-of-plane displacement sensor, a data acquisition system, an extensive data analysis software package, the azimuthal variation of acousto-ultrasonic behavior in graphite/epoxy laminates, and preliminary examination of processing variation in graphite/aluminum tubes.

This Page Intentionally Left Blank

Table of Contents

1.0 Introduction

The acousto-ultrasonic method of nondestructive evaluation is an extremely sensitive means of assessing material response. Efforts continue to complete the understanding of this method. In order to achieve the full sensitivity of the technique, extreme care must be taken in its performance. This report provides an update of the efforts to advance the understanding of this method and to increase its application to the nondestructive evaluation of composite materials. Included are descriptions of a novel optical system that is capable of measuring in-plane and out-of-plane displacements, an IBM PC-based data acquisition system, an extensive data analysis software package, the azimuthal variation of acousto-ultrasonic behavior in graphite/epoxy laminates, and preliminary examination of processing variation in graphite/aluminum tubes.

2.0 Optical Displacement Sensor

A means of quantitatively assessing the out-of-plane and in-plane displacement has been developed because of the uncertainty of the exact nature of the wave propagation associated with the acousto-ultrasonic method.

Michelson-type interferometers are only sensitive to the out-of-plane displacement of the motion of the test surface under strain. In order to be able to measure the in-plane displacements on the test surface, a new speckle interferometer has been designed. The speckle effect is produced when a diffusing surface is illuminated in coherent light. The intensity of the speckle pattern is a random distribution caused by interference of the light amplitudes from all of the

contributing points on the diffusing illuminated area [2]. This effect can also be accomplished by the scattering of light on a retro-reflective diffusing surface area under interrogation. The diffusing surface is made with stick-on sheeting of a high grain retro-reflective material [3]. Scattering grains of similar size on the diffusing adhesive tape can reflect back an incident beam of light to form a diffraction halo, similar to an Airy disk diffraction produced by a circular aperture. The diameter of the diffraction halo at a distance d from the retro-reflective surface is $1.22\lambda d/s$, where s is the size of the speckle grains and λ is the wavelength. In addition, the random spatial distribution of the speckle grains modulates the far-field diffraction pattern with granularity.

In this optical configuration (Fig. 1) the unexpanded laser beam converges by the action of a long focal-length condensing lens. A beamsplitter positioned close to the focusing lens divides the focusing beam into two components. Both focusing beams are directed onto the surface under study by deflecting mirrors located along their paths. The illuminated region of the test surface is covered with a diffusing retro-reflective tape. Due to retro-reflectivity of the illuminated area the speckle pattern formed by each of the beams is seen by the beamsplitter. The beamsplitter spatially superimposes these two identicial speckles and forms the correlation speckle pattern. The speckle grains are considered to be attached to the diffusing tape which in turn adheres to the object surface so that if the object surface is disturbed, the speckle patterns are disturbed, too. Consequently, the motion of the points on the illuminated area causes a variation in the detailed distribution of the correlation speckle pattern. By detecting

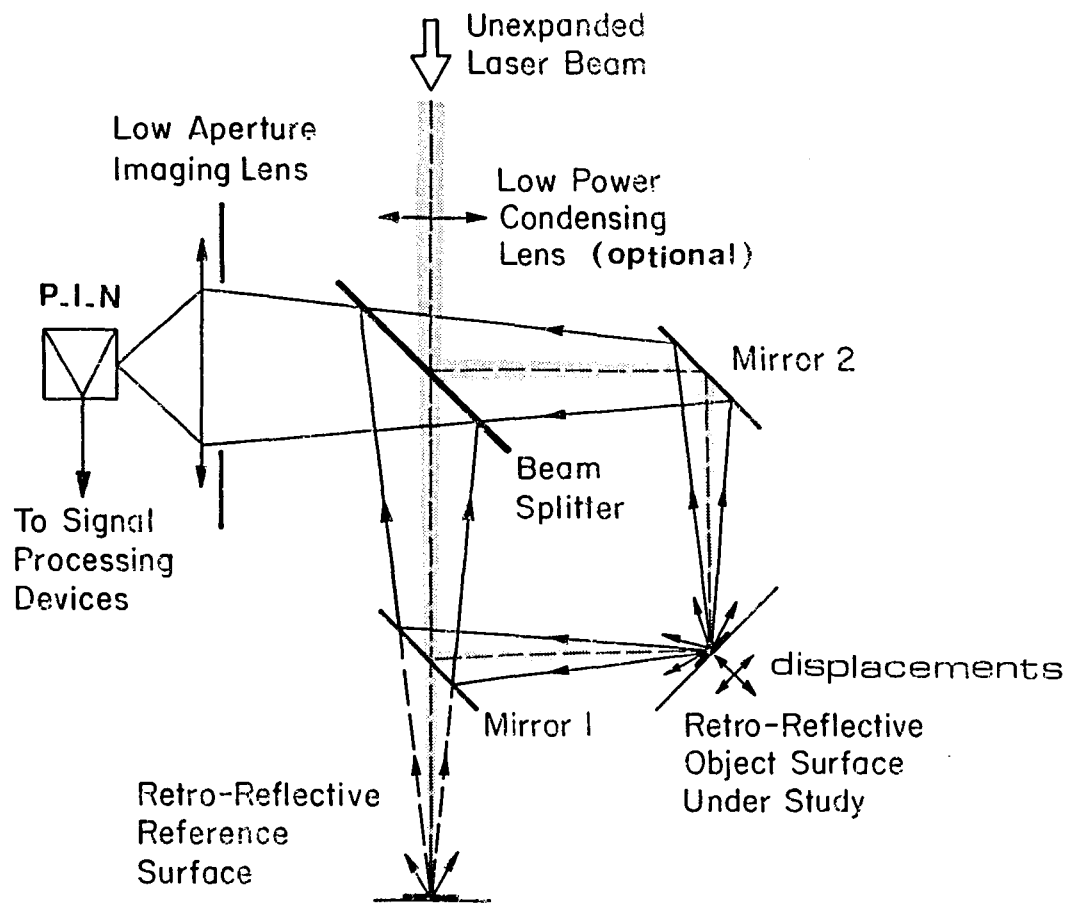

Fig. 1 Retro-reflective speckle interferometric optical configuration for in-plane and out-of-plane displacement detection.

this speckle pattern deformation (twinkling of the combined speckle patterns), the information about the surface displacement amplitudes of the stress wave propagating on the illuminated object surface can be obtained. The optional use of the focusing lens placed next to the beamsplitter facilitates the interrogation of a very small surface area (point-wise detection) and increases the sensitivity to the measured displacement amplitudes. The sensitivity to the acoustic amplitudes depends on the spatial resolution (size) of the focused laser beam. For ultrasonic wave detection, it is required that the diameter of the focused illumination beam be less than the wavelength of the acoustic wave. In other words, the smaller the focused laser beam diameter, the higher the detectable acoustic frequency or the broader the dynamic range. The aperture size of the image-forming lens influences the size of the speckle spots so that the speckle sizes are increased as the light-gathering diameter of the lens is decreased [4]. Since the absolute displacement amplitudes are obtained for object particle displacements of less than the speckle sizes, the production of relatively large speckle patterns insures the linear response of the system.

In the double illuminating arrangement of Fig. 1, the in-plane displacement parallel to the direction of wave propagation is obtained. The displacement is found to be a function of the resultant intensity of two coherently superimposed speckle pattern distributions. This intensity is a function of the phase difference (which in turn is a function of the optical path length difference) introduced by the motion of the speckle pattern [5]. The amplitude of the displacement can be obtained following proper analysis of the

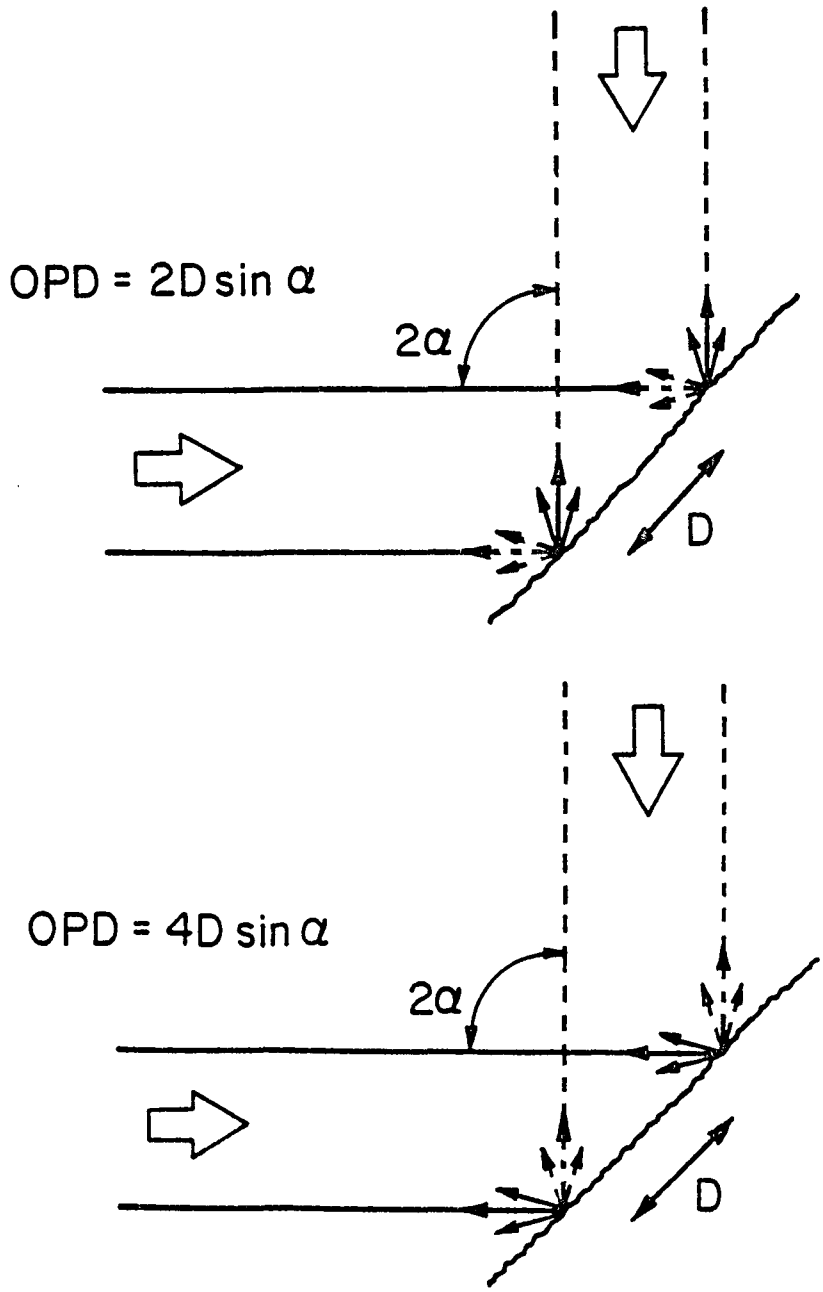

Fig. 2 Comparison of optical path lengths, a) optical path difference for in-plane surface displacement, D, for double-beam illumination of a specularly diffusing surface, b) for a retro-reflective diffusing surface.

photodetector signal in the manner mentioned in Ref. [6]. Due to the angular symmetry of the double illumination beams with respect to the surface normal, only in-plane displacement of the illuminated area gives rise to twice the optical phase change for each beam. Although the normal (out-of-plane) displacement causes two optical phase changes of equal magnitude but opposite sense for the corresponding two beams, the net optical phase change contribution is always zero. By removing mirror 1 and directing the respective beam on a stationary retro-reflective tape, the superposition of two unidentical speckle patterns will be formed. This particular (single illuminating) arrangement is primarily sensitive to the out-of-plane displacement of the test surface. Thus both in-plane and out-of-plane displacement measurements can be accomplished, without disturbing the specimen, by simply removing one of the beam-deflecting mirrors.

Figure 2 shows the resultant optical path length (OPD) for the double-illumination beams on a specular and a retro-reflective surface. Due to the use of diffusing retro-reflective tape in this speckle interferometric arrangement, the sensitivity to the measured displacements is enhanced by a factor of two compared to the conventional speckle displacement interferometers. This arises from the fact that the OPD caused by surface displacements is doubled as a result of retro-reflectivity. The scattered light-gathering capability of this system is also greatly improved as compared to its counterparts in which a lens of finite size aperture is used in forming the two image speckle patterns needed for superposition analysis. Figures 3, 4 show the in-plane and the out-of-plane surface displacements of a PZT ceramic in an experiment using the double and the single illumination arrangements,

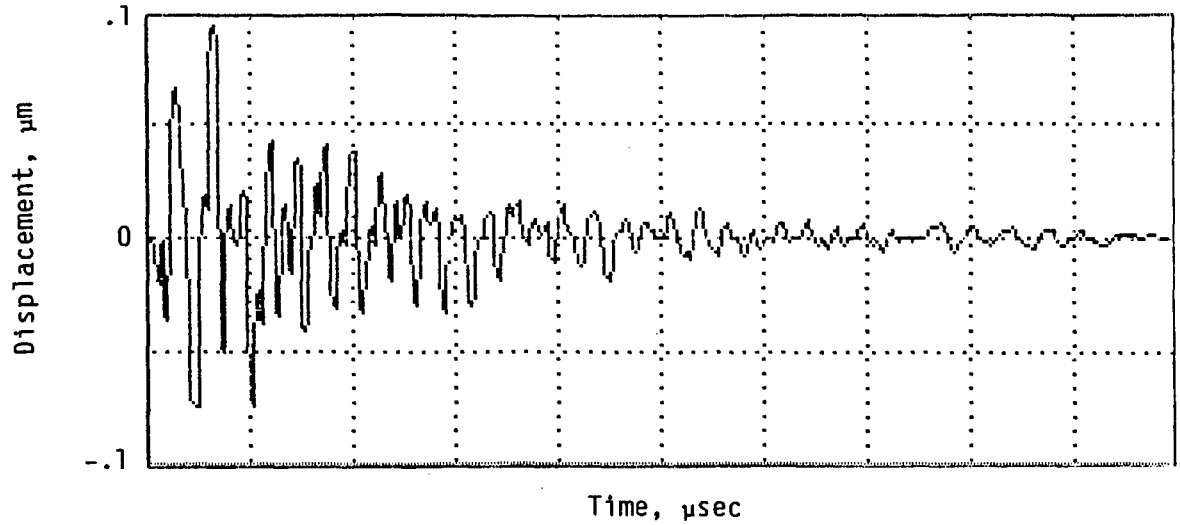

Fig. 3 Observed in-plane displacement of a vibrating PZT transducer using double illumination.

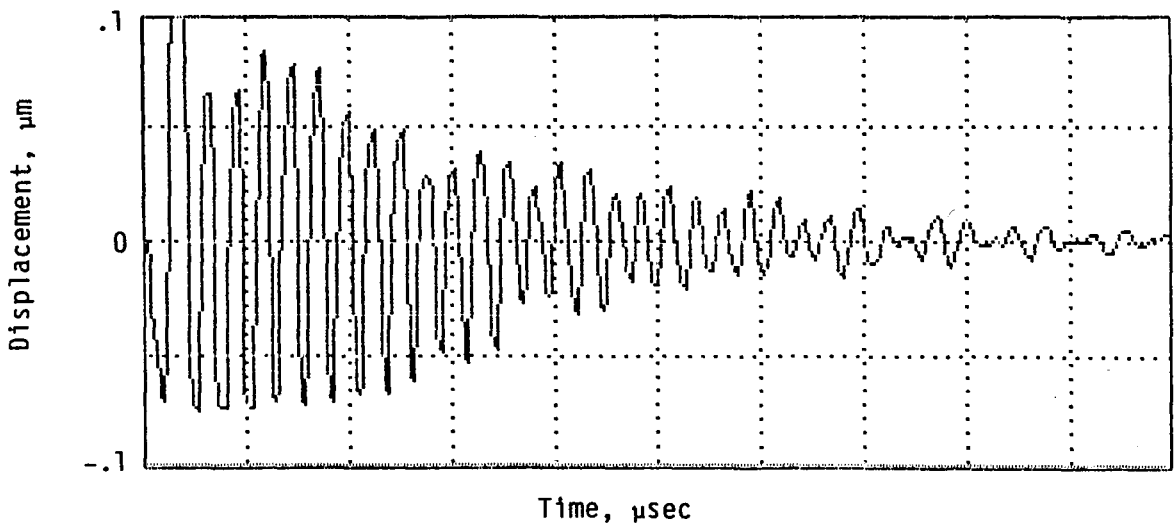

Fig. 4 Observed out-of-plane displacement of a PZT transducer using the single illumination arrangement.

respectively. A complete system analysis and its application in nondestructive evaluation of engineering materials is currently in progress.

The present system can be modified so that the test-piece under study can be isolated from the optical table where the rest of the optical components are located. This flexibility is achieved by replacing the two deflecting mirrors in Fig. 1 with a flexible optical fiber bundle (with associated optical coupling lenses at each fiber end) at each arm. The advantages to optical displacement sensors, with the addition of optical fibers in the noncontacting remote detection of acoustic emission and ultrasonic stress waves in a service environment, are yet to be realized.

3.0 Data Acquisition System

Experimental investigation of materials using ultrasonic methods require examining a large amount of data. In a conventional procedure like ultrasonic C-scanning, such large amounts of data are handled conveniently; only a small portion of the available information is used. In order to effectively evaluate the acousto-ultrasonic behavior, an acquisition system was developed that was capable of capturing the entire detected waveform. Furthermore, because of the desire to examine reasonably large amounts of data and to process it using computerized techniques, an economic means of collection and analysis was sought.

The system finally constructed utilizes an IBM personal computer specially equipped with a PC-DAS board [7]. The board enables the PC to function as a versatile high speed data acquisition system. The system, which may be externally or internally triggered, can sample up to 4096

data points with real-time sampling rates of up to 20 MHz; the system is capable of equivalent time sampling at 160 MHz and averaging of up to 128 signals. Any portion of the captured signal can be viewed or stored for analysis with fast fourier transforms (FFT) of portions up to 512 points available with a single key stroke. Hard copies of the stored signal or FFT may be made using a dot matrix printer. Once the signals have been stored on a diskette file they may be analyzed more extensively once sampling has been completed. Using the IBM PC has sacrificed data analysis computational speed, but the acquisition speed is maintained and the overall convenience is significantly greater than with use of a mainframe computer.

4.0 Data Analysis Software

In order to extract as much information as possible from the detected signals, as well as to allow for comparison of signals one with another, a special software program was developed. Figures 5 and 6 are flowcharts of the main program and a plotting program, respectively.

The features of the main software package, Fig. 5, include:

1) Can digitally gate and display an inputted (detected) time-domain signal.
2) Can make time/voltage data average zero.
3) Can perform Fast Fourier Transform (FFT) on original or gated time-domain signal.
4) Can calculate transfer function from selectable input and output signals.
5) Can digitally filter FFT data.

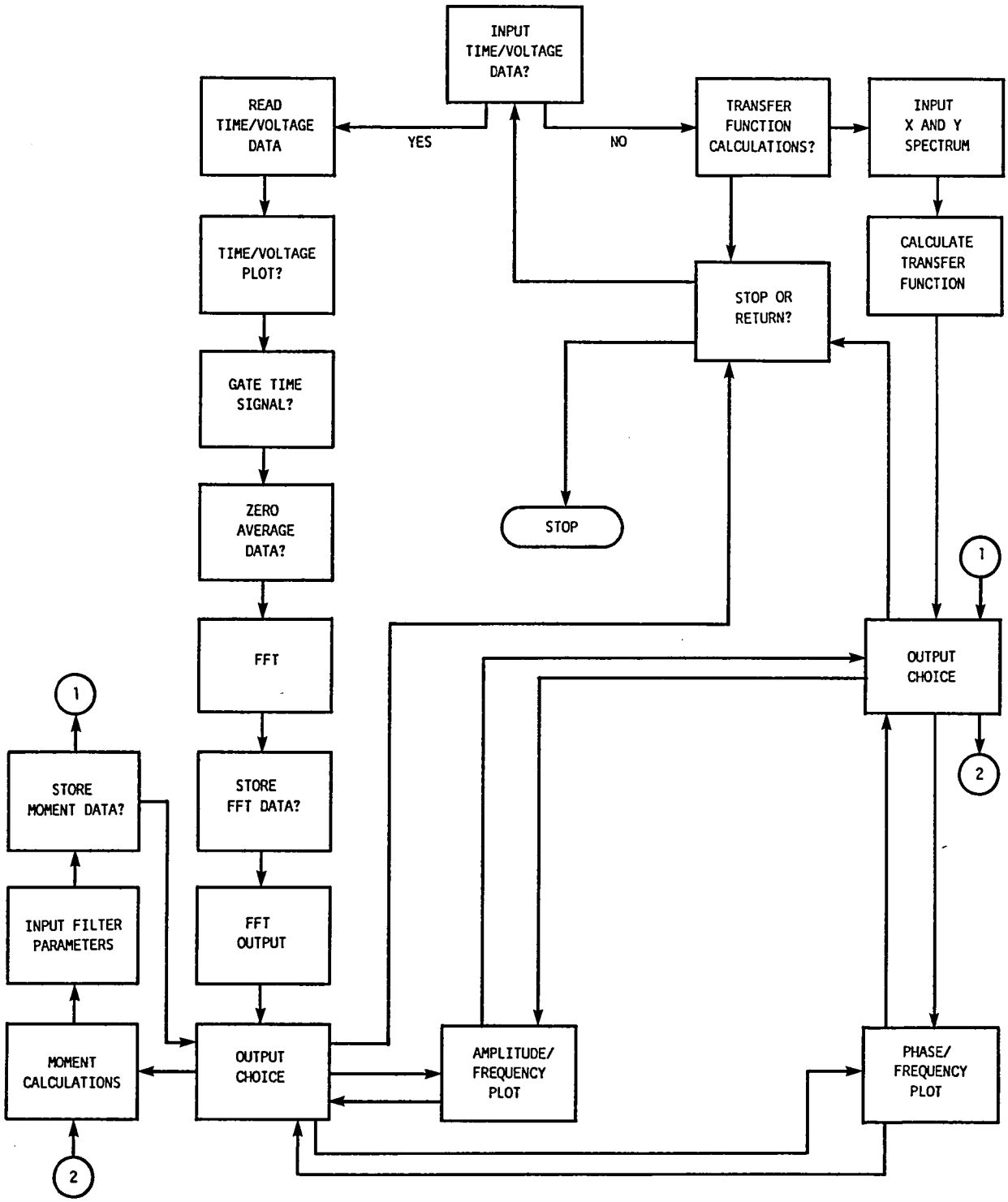

Fig. 5 Flowchart of main signal analysis software package.

6) Can display amplitude/frequency or phase/frequency plots of both immediate FFT data or transfer function data.

7) Can calculate SWF parameters [8] (i.e., shape parameters) on filtered or unfiltered FFT data or transfer function data.

8) All SWF calculations can be stored on disk for easy access for plotting.

9) Can select maximum and minimum values on plots so easy comparison can be made between different data.

10) Can compress or expand the x-axis to improve examination of various features of the data.

11) Allows for use of the cursor control to find frequency peaks.

A program, Fig. 6, has been written to automatically generate SWF parameters versus azimuthal angle plots. All software is user friendly and automated for as little time expenditure as possible for the user.

5.0 Variation of Acousto-Ultrasonic Behavior with Aximuthal Angle

In any study of fundamental behavior it is imperative that a systematic approach be established; it may be necessary from time to time to alter the approach based on findings. The initial approach taken in the work under way in the Materials Response Laboratory at Virginia Tech has as its basis the following concept: In that laminated fiber reinforced composite materials are composed of laminae and the specific combination, in fact even the individual laminae, are influenced in this mechanical performance by constraint, a fundamental (sometimes called critical) element has been identified. That is to say, a particular lamina has been selected for observation when

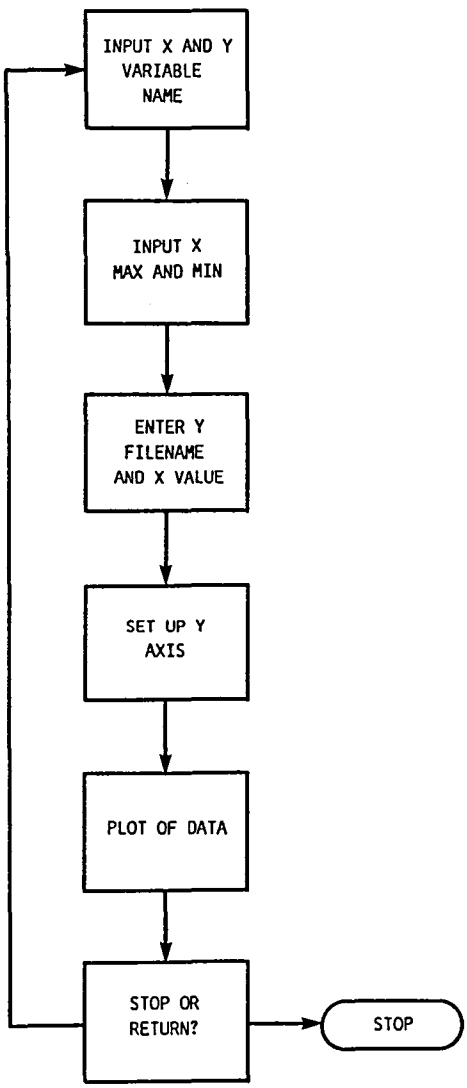

Fig. 6 Flowchart of software package used to generate data plots.

subjected to a variety of constraint situations. Initially a "0 degree lamina" laminated within a $[0_2]_s$ laminate, a $[45/0]_s$, and a $[90/0]_s$ laminate have been considered. (Of course, the description of "0 degree" is arbitrary but significant.) The laminates included subject the fundamental element to differing states of constraint; this is easily evidenced by consideration of the predicted deformation obtained by classical lamination theory for various states of applied stress. The in-plane constraint in any of these situations is clearly dependent on direction. Consequently the acousto-ultrasonic behavior has been studied as a function of azimuthal angle. Since most techniques for performing the acousto-ultrasonic measurement involve two transducers placed in different locations on the object, a number of possible ways of examining the azimuthal variation are possible. The work here has considered the region of interest to be that region located between the transducers, consequently in this study both transducers were moved.

By carefully mapping a set of radial fiduciary marks, the specially modified transducer spacing fixture provided precise orientation at 5 degree intervals. The output voltage of the receiving transducer as a function of time at each location was captured and a number of consecutive received signals were averaged. The time-domain signals, although retained, are not provided, since direct examination is typically inconclusive. The corresponding amplitude versus frequency plots for the $[0_2]_s$ laminate are shown (Fig. 7 a-m); they are not included for the other two laminates studied.

Attention is drawn in particular to the low frequency peak (approximately 1 MHz) and the high frequency peak (approximately 3.5 MHz). Justification for identifying these features as "peaks" is

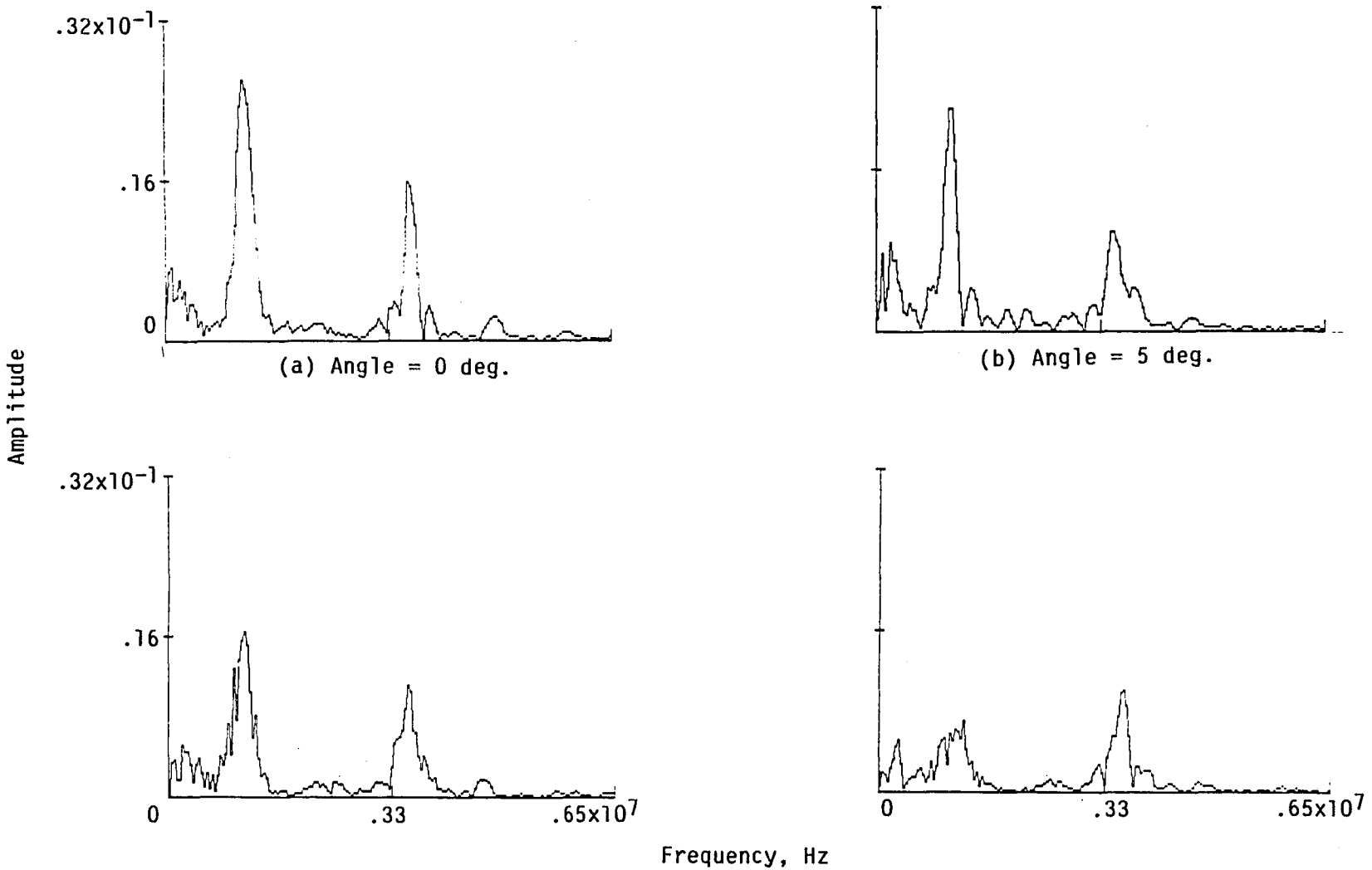

Fig. 7 Amplitude versus frequency plots for various azimuthal orientations.

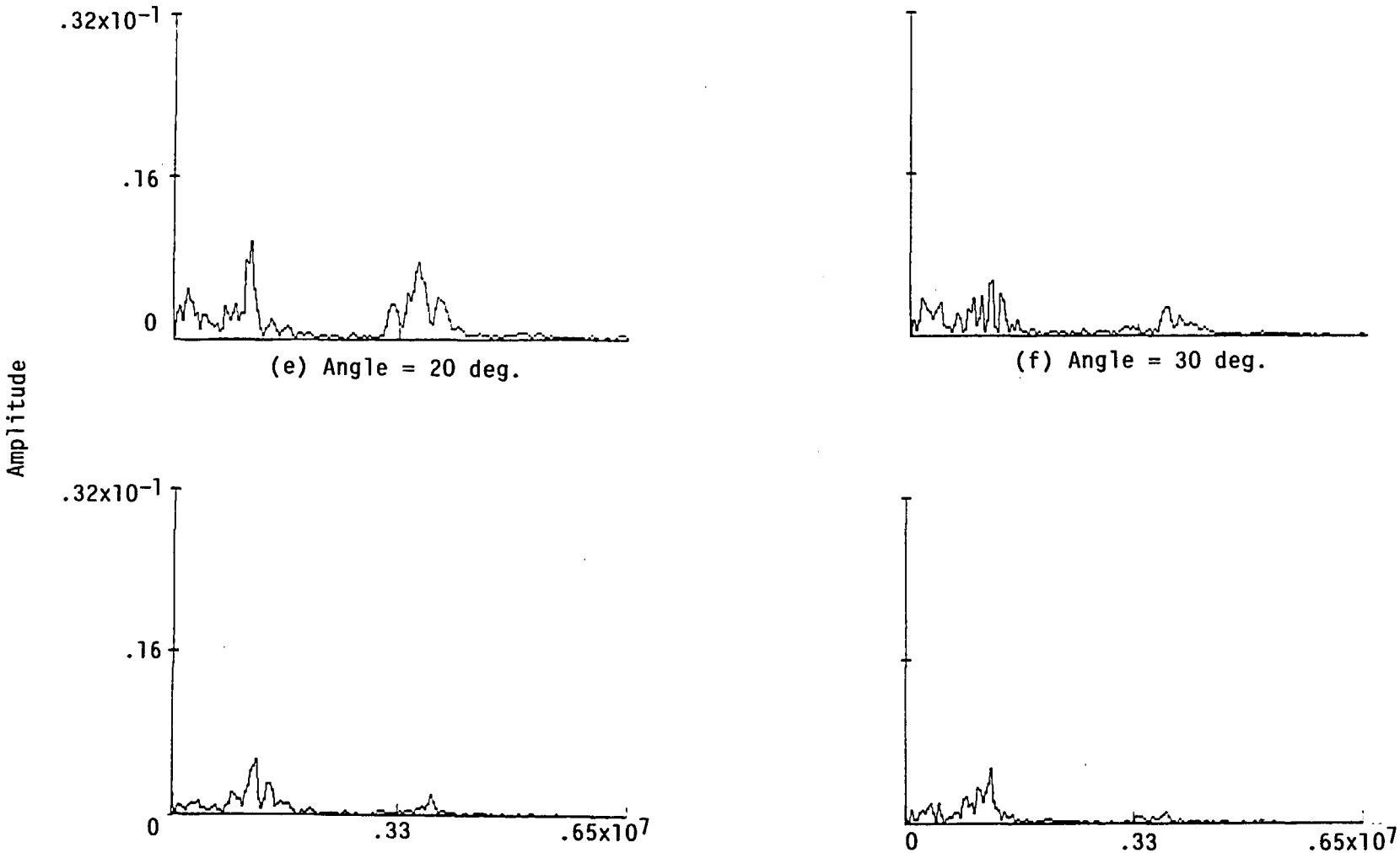

Fig. 7 Continued.

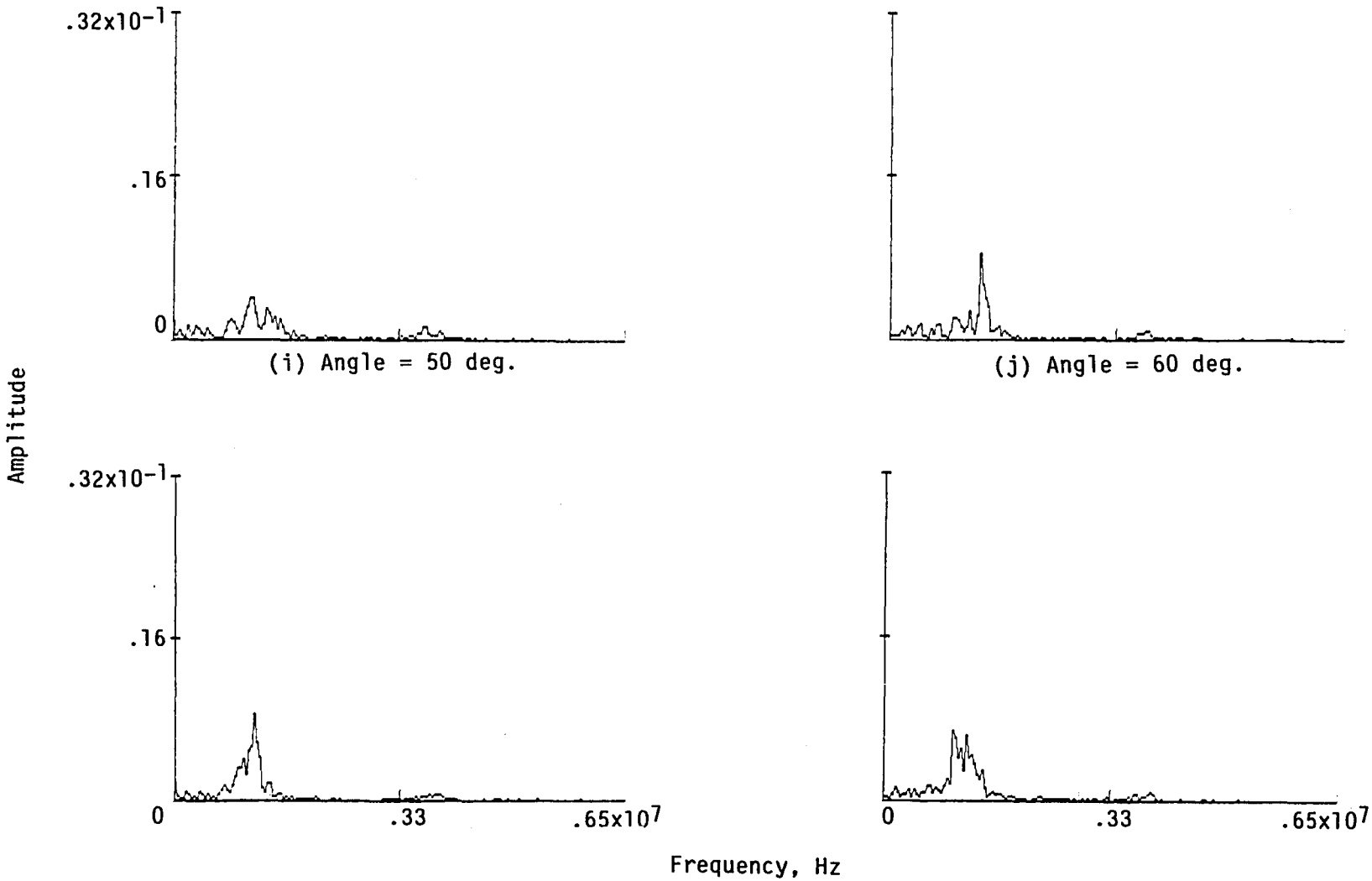

Fig. 7 Continued.

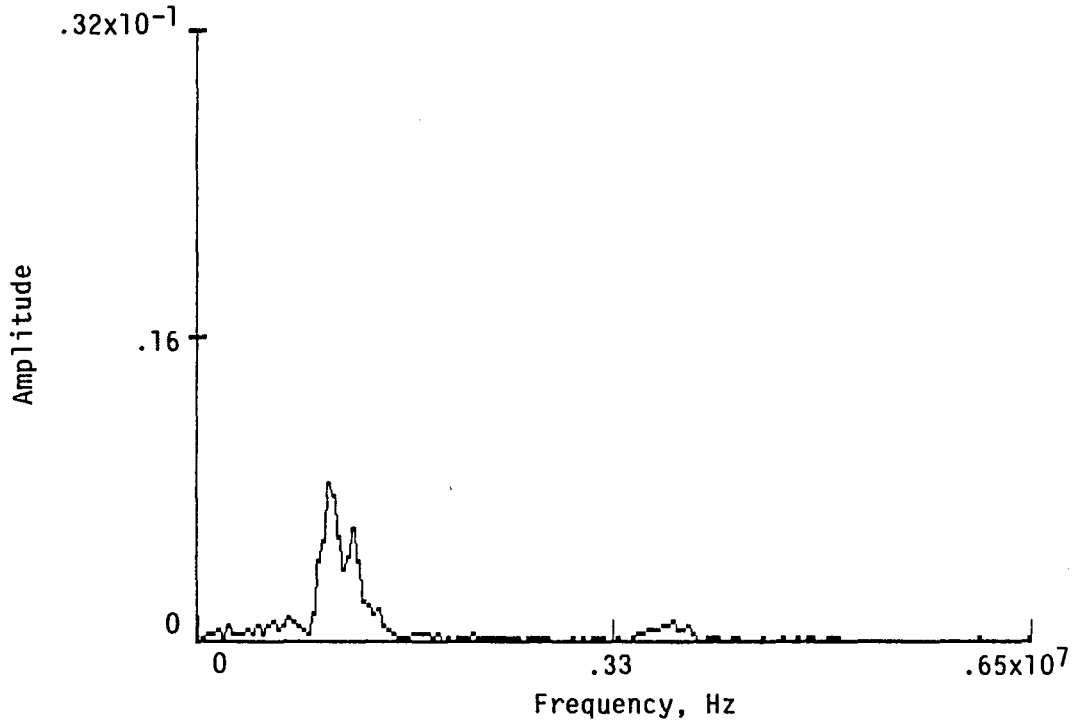

(m) Angle = 90 deg.

Fig. 7 Concluded.

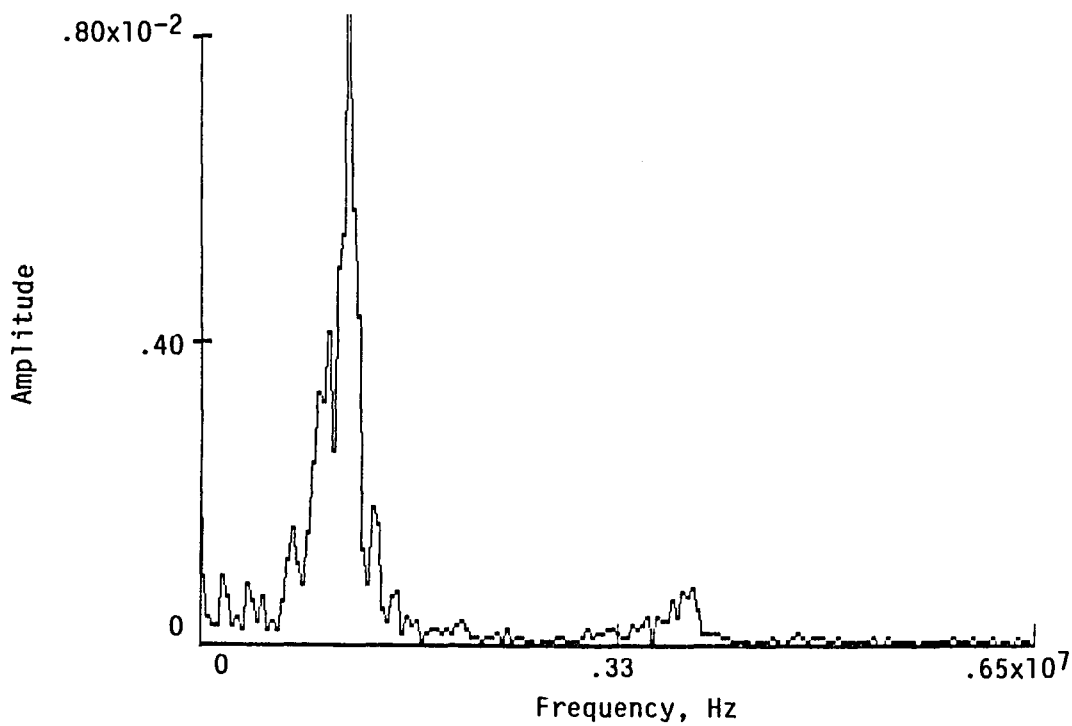

Fig. 8 Amplitude versus frequency plot of data displayed in Fig. 7(k) with magnified amplitude scale.

provided in Fig. 8 which displays the data corresponding to Fig. 7k with a magnified amplitude scale.

Whereas visual comparison suggests a variety of features, a quantitative comparison is difficult. It was precisely for this purpose that the scheme for quantifying the acousto-ultrasonic spectrum in terms of SWF parameters or moments was adopted. This procedure has been discussed previously [8], and for convenience they are stated here, after the notation of Talreja:

$$SWF1 = M_0 \text{ (Area)}$$

$$SWF2 = \frac{M_1}{M_0} \text{ (Centroid) where}$$

$$M_r = \int_{f_i}^{f_f} A(f)\, f^r df$$

f_i - initial frequency

f_f - final frequency

$A(f)$ - Amplitude Spectral Distribution

Figure 9 is a plot of SWF1 versus azimuthal angle which indicates a rather rapid decrease until 45 degrees and a modest increase from there until 90 degrees; this measure is related to energy. Figure 10 shows the variation of SWF2 with angle and suggests that the center frequency (centroid) increases until 20 degrees and then decreases. Since it is reasonably evident that the relative energy of the high frequency and low frequency portions are dominating this behavior, Fig. 11 was developed. In this case the moment calculations were performed using an

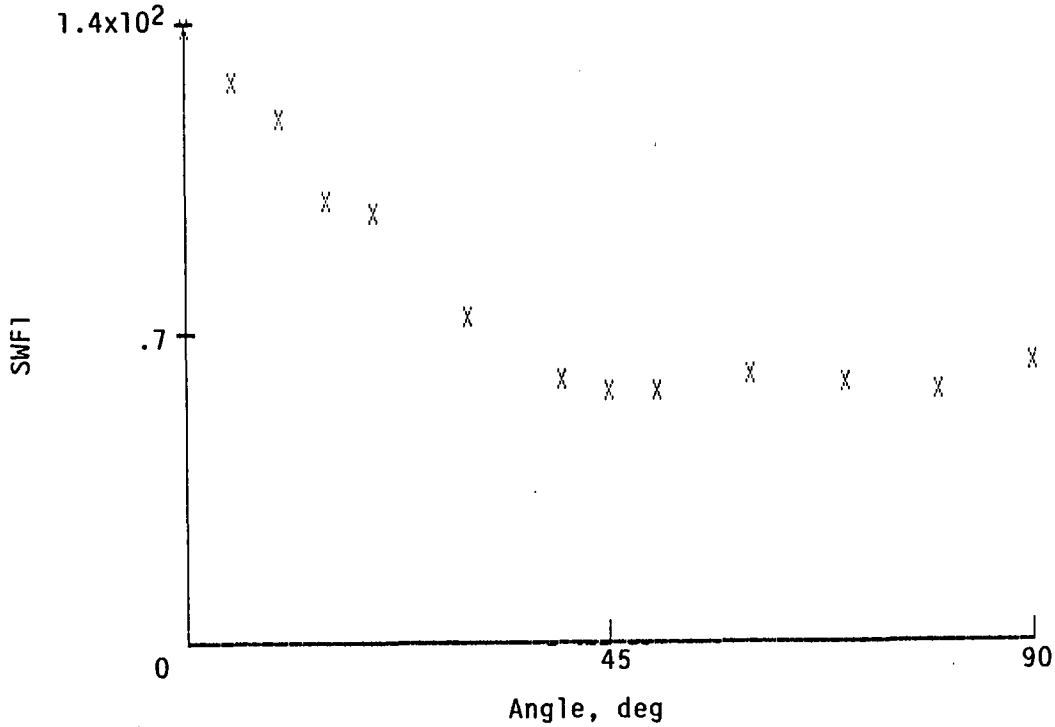

Fig. 9 Plot of SWF1 versus azimuthal angle, $[0_2]$s laminate.

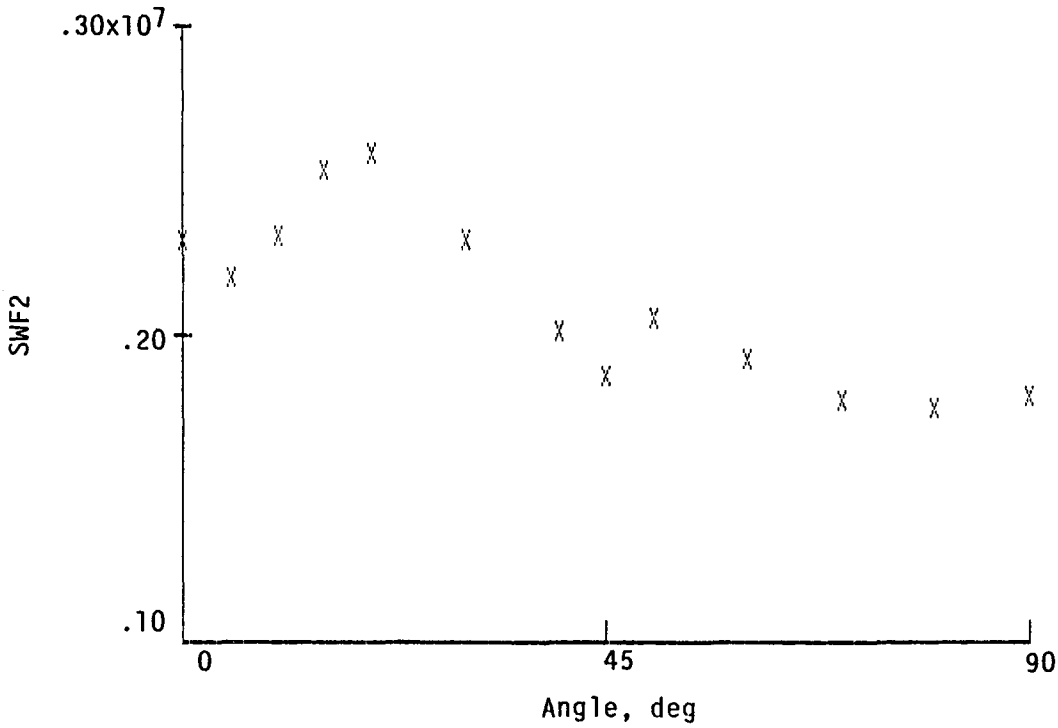

Fig. 10 Plot of SWF2 versus azimuthal angle, $[0_2]$s laminate.

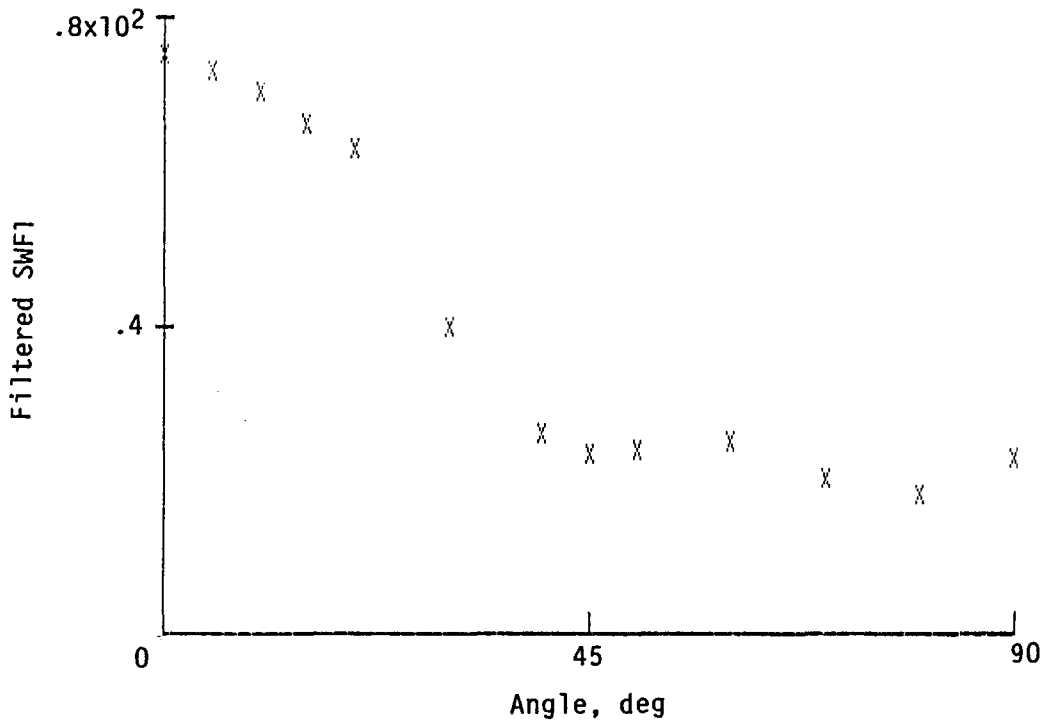

Fig. 11 Plot of SWF1 versus azimuthal angle after each spectrum has been filtered, $[0_2]s$ laminate.

initial frequency of 2.5 MHz and a final frequency of 5.0 MHz; the behavior reflected is that of only the high frequency.

At this time the observed behavior appears in part to be the result of Lamb wave modes of vibration, the low frequency part. The high frequency has not yet been explained.

Figures 12-14 are the corresponding plots for the $[90/0]_s$ laminate. An explanation of these observations involving the superposition of the behavior of a 0-degree laminate with a 90-degree laminate seems plausible.

Figures 15-17 are the corresponding plots for the $[45/0]_s$ laminate. Superposition appears insufficient, or inappropriate, to explain these observations.

Efforts to explain the fundamental nature of the acousto-ultrasonic wave propagation and the cause for its variation with constraint continues. Work involving experimental observation of the effects of various forms of load induced damage is also under way. Laminates containing artificial "delaminations" are being studied along with laminates containing various amounts of matrix cracking.

6.0 Preliminary Evaluation of Processing Variations in Graphite Fiber/Aluminum Matrix Tubes

A number of graphite/aluminum metal matrix composite tubes manufactured by MCI, Inc. of Columbus, Ohio were examined in an effort to determine the sensitivity of the acousto-ultrasonic method to variations in processing and, in one instance, applied load. The geometry posed an initial complication that was overcome by the use of plexiglass waveguides. Measurements of the acousto-ultrasonic behavior

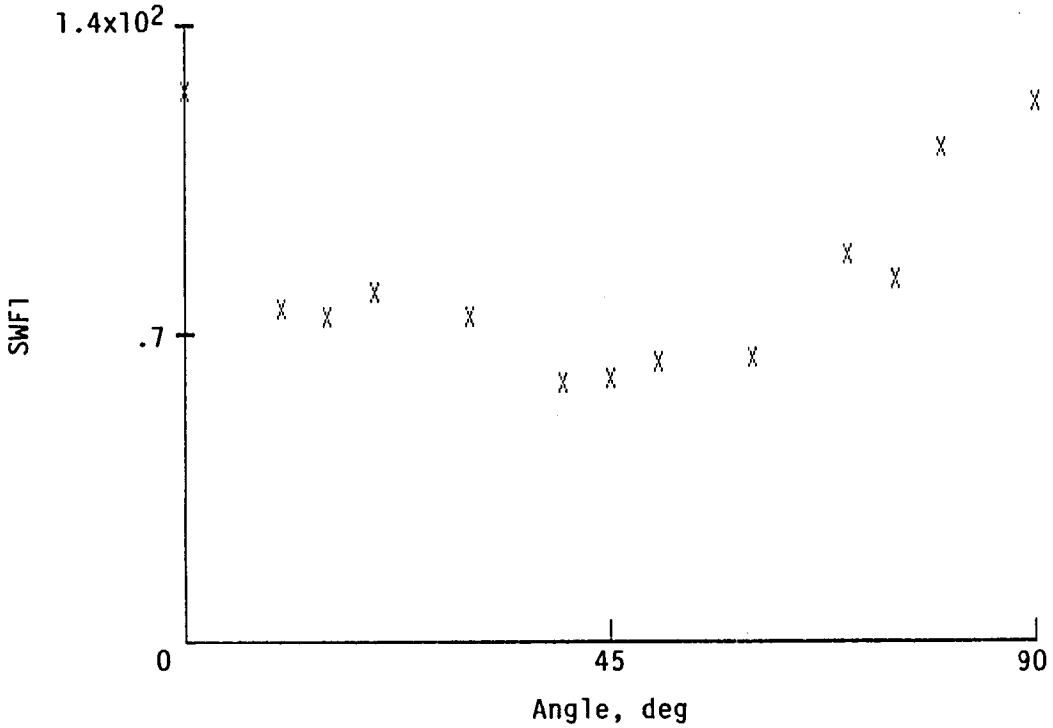

Fig. 12 Plot of SWF1 versus azimuthal angle, [90/0]s laminate.

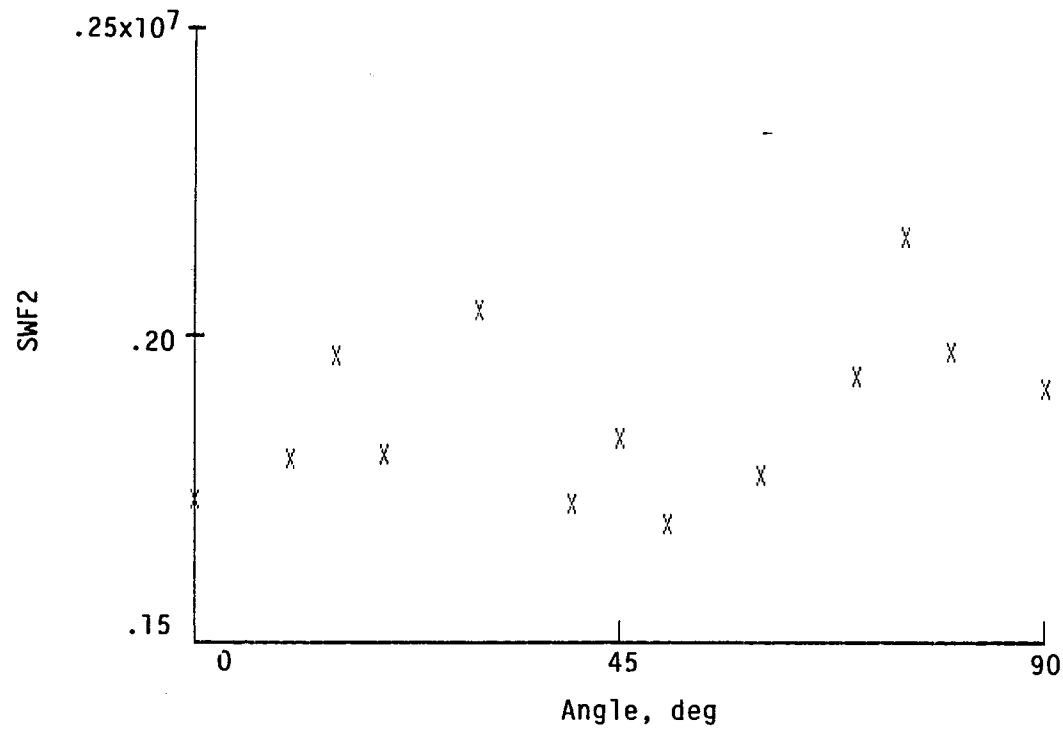

Fig. 13 Plot of SWF2 versus azimuthal angle, [90/0]s laminate.

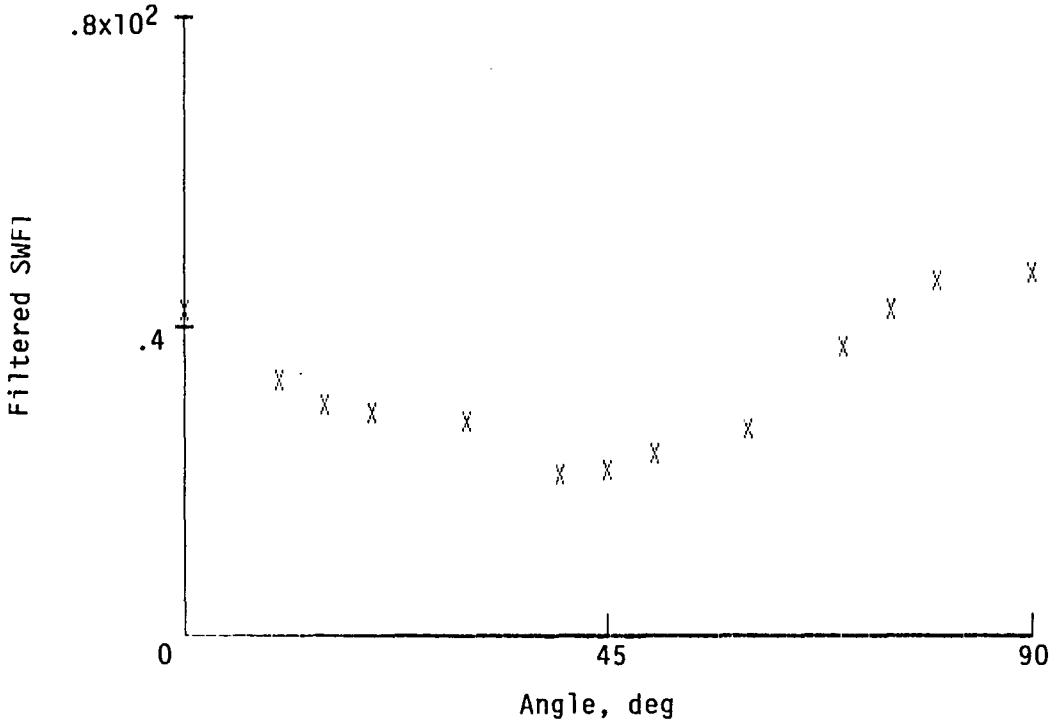

Fig. 14 Plot of SWF1 versus azimuthal angle after each spectrum has been filtered, [90/0]s laminate.

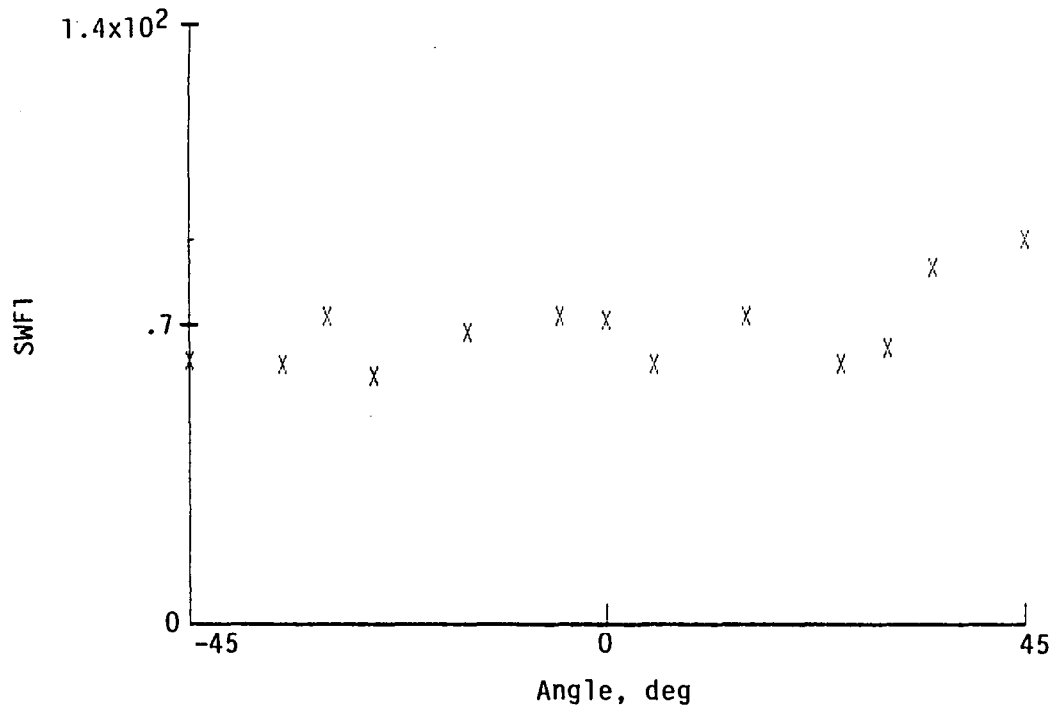

Fig. 15 Plot of SWF1 versus azimuthal angle, [45/0]s laminate.

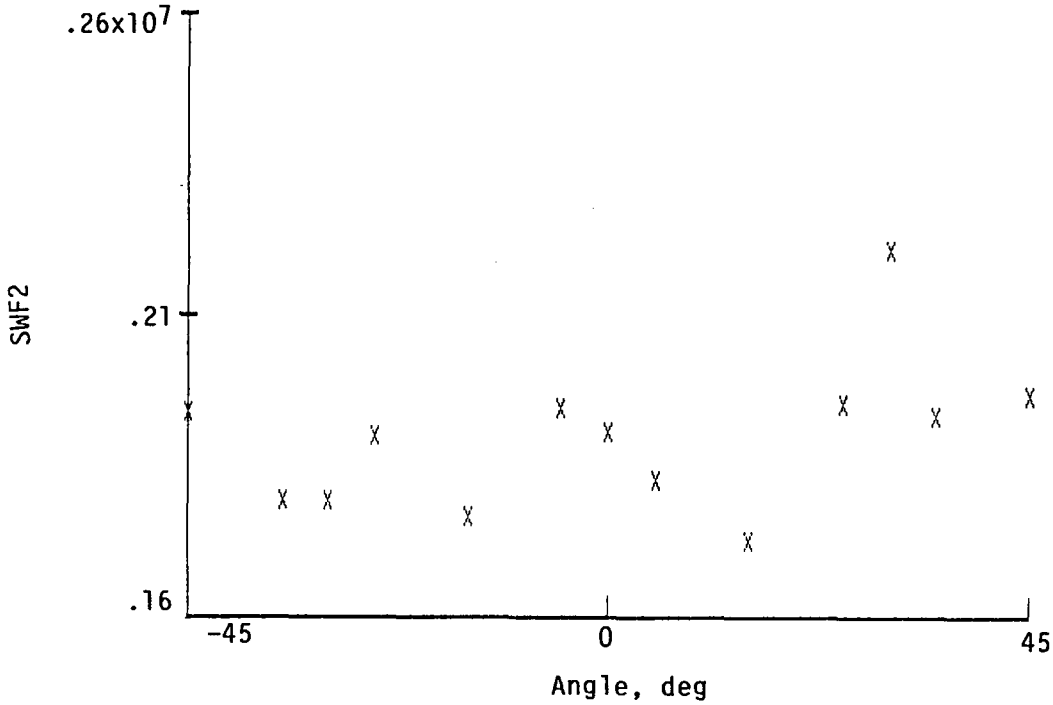

Fig. 16 Plot of SWF2 versus azimuthal angle, [45/0]s laminate.

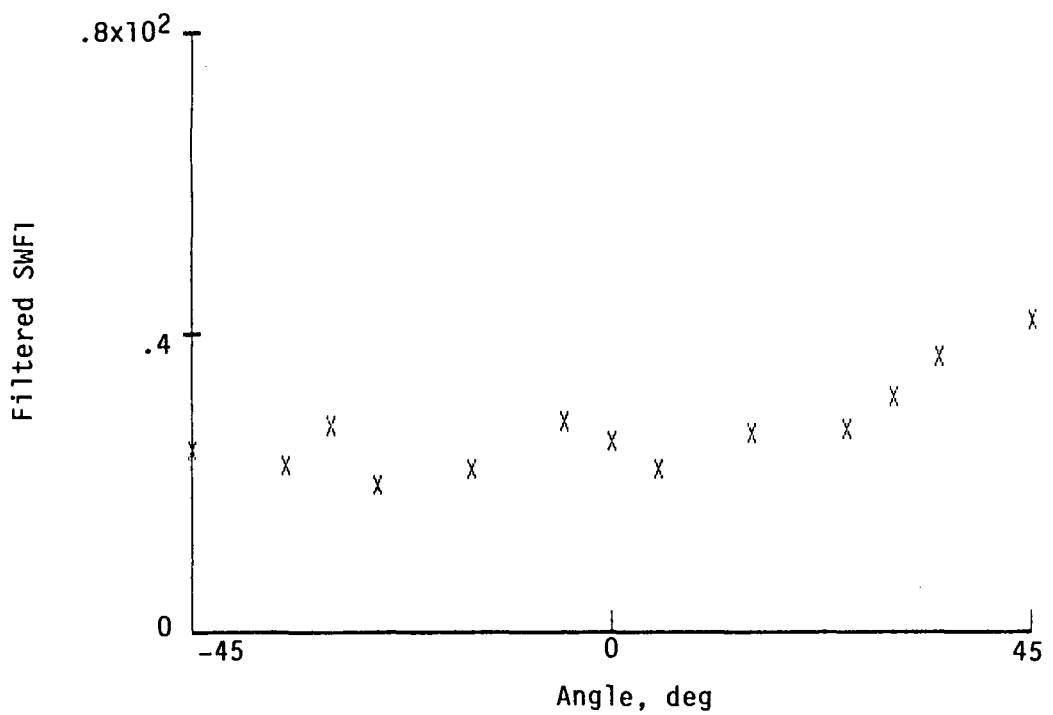

Fig. 17 Plot of SWF1 versus azimuthal angle after each spectrum has been filtered, [45/0]s laminate.

were made with the transducers separated in the axial direction and also with them separated in the radial direction. These two configurations were considered because of the method used for forming the tubes.

On a limited number of samples the following was observed:

i. variations from place to place along the same tube, Fig. 18,

ii. progressive variation along the length of the same tube,

iii. differences from tube to tube of the same type,

iv. differences between "virgin" and mechanically loaded tubes, Fig. 19,

v. variations from place to place around the tubes, believed to be caused by clad overlay seams.

More work is needed to completely define the nature and significance of these observations, as well as to further assess the potential of the acousto-ultrasonic technique.

7.0 Accomplishments

A unique in-plane/out-of-plane optical displacement sensors has been developed and is being applied.

A versatile data acquisition and analysis system has been assembled and is being utilized for studying materials response.

A systematic study of the sensitivity of the acousto-ultrasonic behavior to composite materials without and with damage is under way.

Preliminary examination of Gr/Al tubes indicates a significant potential for the application of the acousto-ultrasonic method to assessing processing variations that could affect mechanical performance.

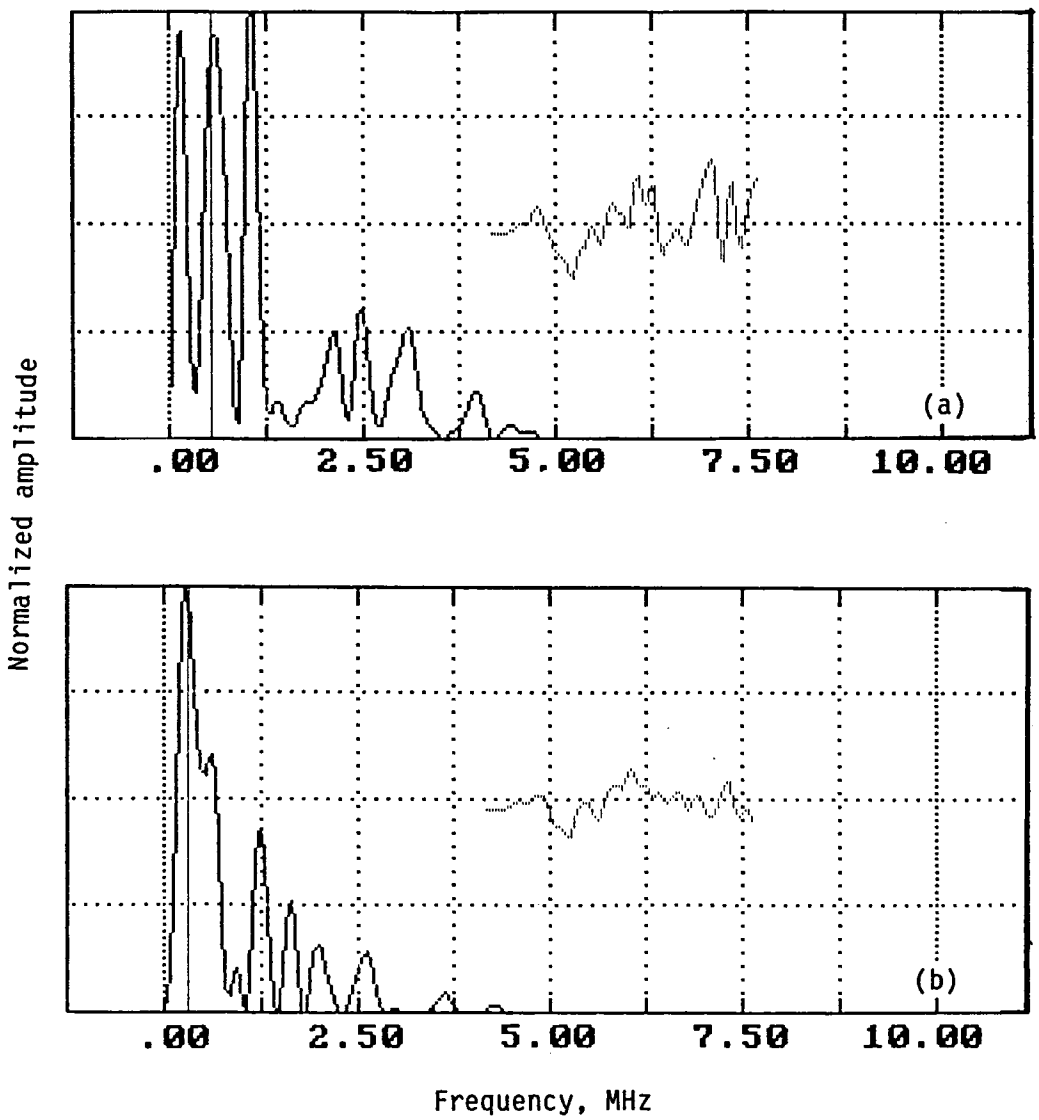

Fig. 18 a) Spectrum of the detected signal in the vicinity of a clad overlay seam. b) Typical spectrum of other regions of the same tube as a). Note: This tube failed at the location from which the a) signal was obtained. The failure appeared to be caused by lack of consolidation.

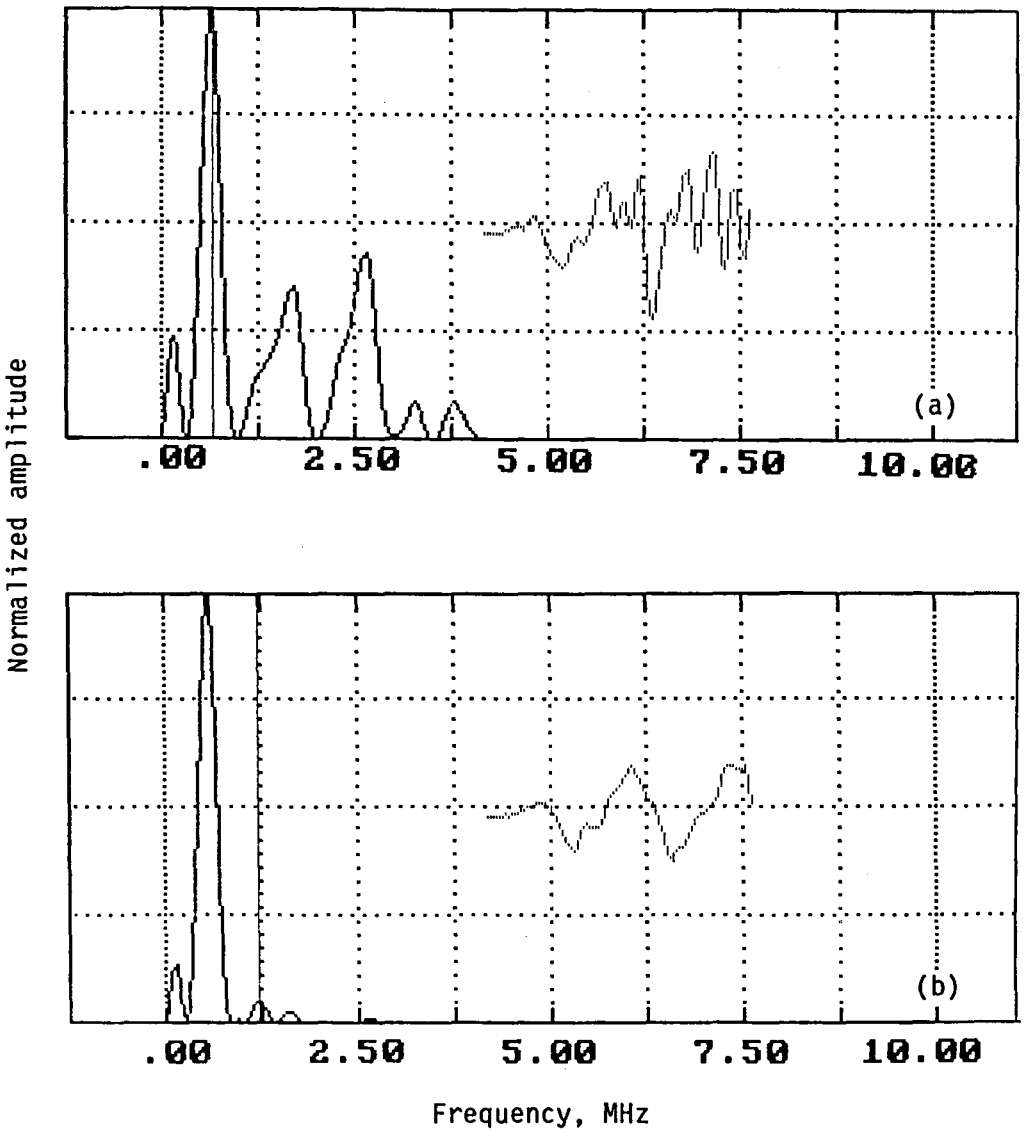

Fig. 19 a) Spectrum of the detected signal in the vicinity of the clad overlay seam in a tube that has been loaded, b) Typical spectrum of other regions of the same tube as a). Note: The tubes examined, fig. 18 and 19, were similar except the latter had been loaded in tension prior to examination.

8.0 References

1. A. Sarrafzadeh-Khoee and J.C. Duke, Jr., "NDE of Engineering Materials Using Ultrasound: Simple Optical Sensor & Fiber Optics Interferometric Application," to be published.

2. J.C. Wyant, "Speckle," in McGraw Hill Encyclopedia of Science and Technology, 12, 1982, pp. 852-853.

3. D.A. Palmer, "Retro-Reflective Materials and Optical Imaging," Appl. Opt., 24 No. 10, May 1985, pp. 413-414.

4. C. Froely, "Speckle Phenomenon and Some of Its Applications," Proc. IUTAM Symp., Optical Methods in Mechanics of Solids, Poitiers, France, 1979, pp. 279-313.

5. D. Joyeux and S. Lowenthal, "Real-Time Measurement of Angstrom Order Transverse Displacement or Vibrations, by Use of Laser Speckle," Opt. Commun., 4, Oct. 1971, pp. 108-112.

6. H. Bahadur and R. Parshad, Physical Acoustics--Principles and Methods, XVI, (W.P. Mason and R.N. Thurston, eds., Academic Press) p. 119.

7. PC-DAS, IBM PC compatible high speed data acquisition board, Adaptronics Products (General Research Corp.) McLean, VA.

8. A.K. Govada, J.C. Duke, Jr., E.G. Henneke, II and W.W. Stinchcomb, "A Study of the Stress Wave Factor Technique for the Characterization of Composite Materials," NASA Contractor Report 174870, Feb. 1985.

1. Report No.	2. Government Accession No.	3. Recipient's Catalog No.
NASA CR-4002		

4. Title and Subtitle	5. Report Date
A Study of the Stress Wave Factor Technique for Nondestructive Evaluation of Composite Materials	July 1986
	6. Performing Organization Code

7. Author(s)	8. Performing Organization Report No.
A. Sarrafzadeh-Khoee, M.T. Kiernan, J.C. Duke, Jr., and E.G. Henneke II	None
	10. Work Unit No.

9. Performing Organization Name and Address	11. Contract or Grant No.
Virginia Polytechnic Institute and State University Dept. of Engineering Science and Mechanics Blacksburg, Virginia 24061-4899	NAG3-172
	13. Type of Report and Period Covered
	Contractor Report

12. Sponsoring Agency Name and Address	14. Sponsoring Agency Code
National Aeronautics and Space Administration Washington, D.C. 20546	506-53-1A 505-90-28 (E-3081)

15. Supplementary Notes

Final report. Project Manager, Alex Vary, Structures Division, NASA Lewis Research Center, Cleveland, Ohio 44135.

16. Abstract

The acousto-ultrasonic method of nondestructive evaluation is an extremely sensitive means of assessing material response. Efforts continue to complete the understanding of this method. In order to achieve the full sensitivity of the technique, extreme care must be taken in its performance. This report provides an update of the efforts to advance the understanding of this method and to increase its application to the nondestructive evaluation of composite materials. Included are descriptions of a novel optical system that is capable of measuring in-plane and out-of-plane displacements, an IBM PC-based data acquisition system, an extensive data analysis software package, the azimuthal variation of acousto-ultrasonic behavior in graphite/epoxy laminates, and preliminary examination of processing variation in graphite-aluminum tubes.

17. Key Words (Suggested by Author(s))	18. Distribution Statement
Nondestructive testing; Ultrasonics; Acousto-ultrasonics; Laser ultrasonics; Stress waves; Stress wave factor; Composites	Unclassified - unlimited STAR Category 38

19. Security Classif. (of this report)	20. Security Classif. (of this page)	21. No. of pages	22. Price*
Unclassified	Unclassified	32	A03

*For sale by the National Technical Information Service, Springfield, Virginia 22161

NASA-Langley, 1986

End of Document